

Supporting information

Molecular orientation dynamics triggers ferroelectricity and ferroelasticity in an organic-inorganic halide material

Hao-Fei Ni, Jia-He Lin, Chang-Feng Wang, Qing-Feng Luo, Pei-Zhi Huang, Zhi-Xu Zhang,* Da-Wei Fu,* and Yi Zhang*

Institute for Science and Applications of Molecular Ferroelectrics, Key Laboratory of the Ministry of Education for Advanced Catalysis Materials, Zhejiang Normal University, Jinhua, 321004, China.

*Corresponding authors: Zhi-Xu Zhang (email: zhangzhixu@zjnu.edu.cn); Da-Wei Fu (email: dawei@zjnu.edu.cn); Yi Zhang (email: yizhang1980@seu.edu.cn)

Experimental Measurement Methods

Synthesis

All reagents and solvents used in this work were obtained from commercial suppliers and were not further purified (PbBr_2 99%, imidazolium 99%, HBr 40 wt % in H_2O). Imidazole (12 mmol) and PbBr_2 (3 mmol) in the ratio 4:1 were dissolved in excess hydrobromic acid solution (25 ml) with stirring at room temperature. After stirring 30 min, a clarified solution was obtained. Crystals were harvested after evaporation of the clarified solution for a week at room temperature and washed by ethyl acetate (total yield: 75-80% based on PbBr_2).

Single crystal X-ray crystallography

Variable-temperature single-crystal XRD data of IM_3PbBr_5 were collected using a Bruker D8 Venture diffractometer with Mo $K\alpha$ radiation ($\lambda = 0.71073 \text{ \AA}$) (operating at 50 kV and 1.4 mA) at different temperature. The processing was disposed by the APEX3. Solve and refine of single crystal data by using SHELXTL and OLEX 1.5 software packages, all non-hydrogen atoms are anisotropically manipulated. Other relevant crystallographic data are listed in Tables S1-S4. CCDC 2253377-2253379 for the compounds contains the supplementary crystallographic data for this article.

Differential scanning calorimetry and dielectric measurements

12.6 mg powder samples of IM_3PbBr_5 were weighed for DSC measurement by NETZSCH DSC 200F3 instrument in a nitrogen atmosphere. The range of heating and cooling processes program is 110 K to 440 K with a rate parameter of 20 K min^{-1} . Complex dielectric constants measurement were performed on the Tonghui TH2828A

instrument over the frequency range of 1 KHz to 1 MHz. The crystal of IM_3PbBr_5 pasted with silver conducting glue was used in dielectric measurements.

Ferroelectric measurement

The direction of the polar axis of the crystal was determined by anisotropic dielectric measurements. Then, the measured sample was prepared by coating with conductive silver glue on each sides of the polar axis of the IM_3PbBr_5 crystal. P - E hysteresis loops of prepared sample were measured on Radiant Precision Premier II with a typical Sawyer-Tower circuit.

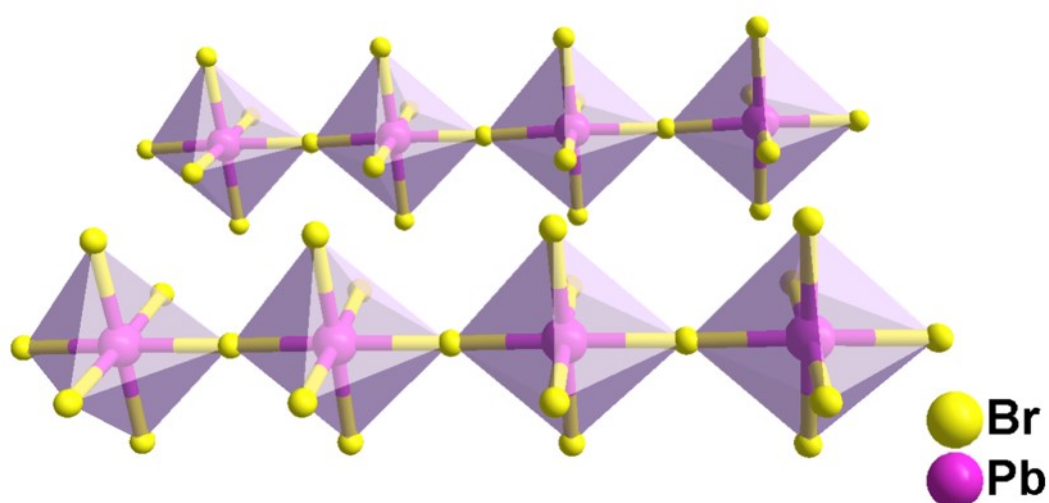


Fig. S1 The corner-sharing $[\text{PbBr}_5]^{3-}$ infinite 1D anionic chains in IM_3PbBr_5 .

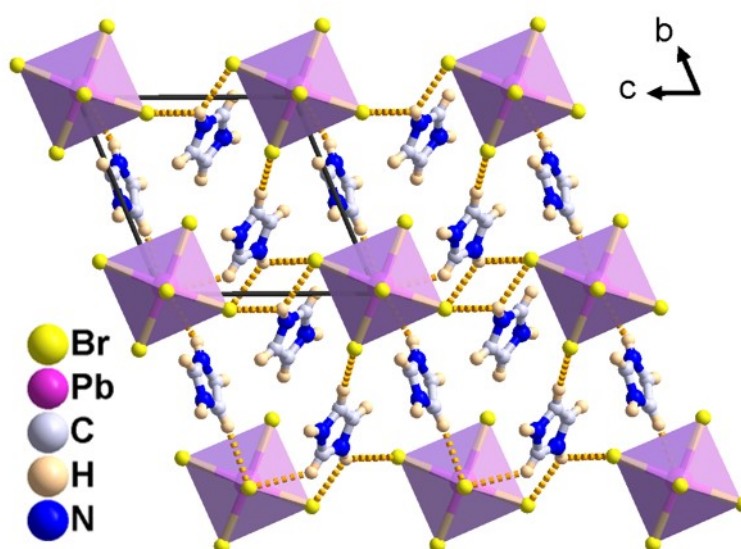


Fig. S2 Hydrogen bonds of IM_3PbBr_5 at 120 K in LTP.

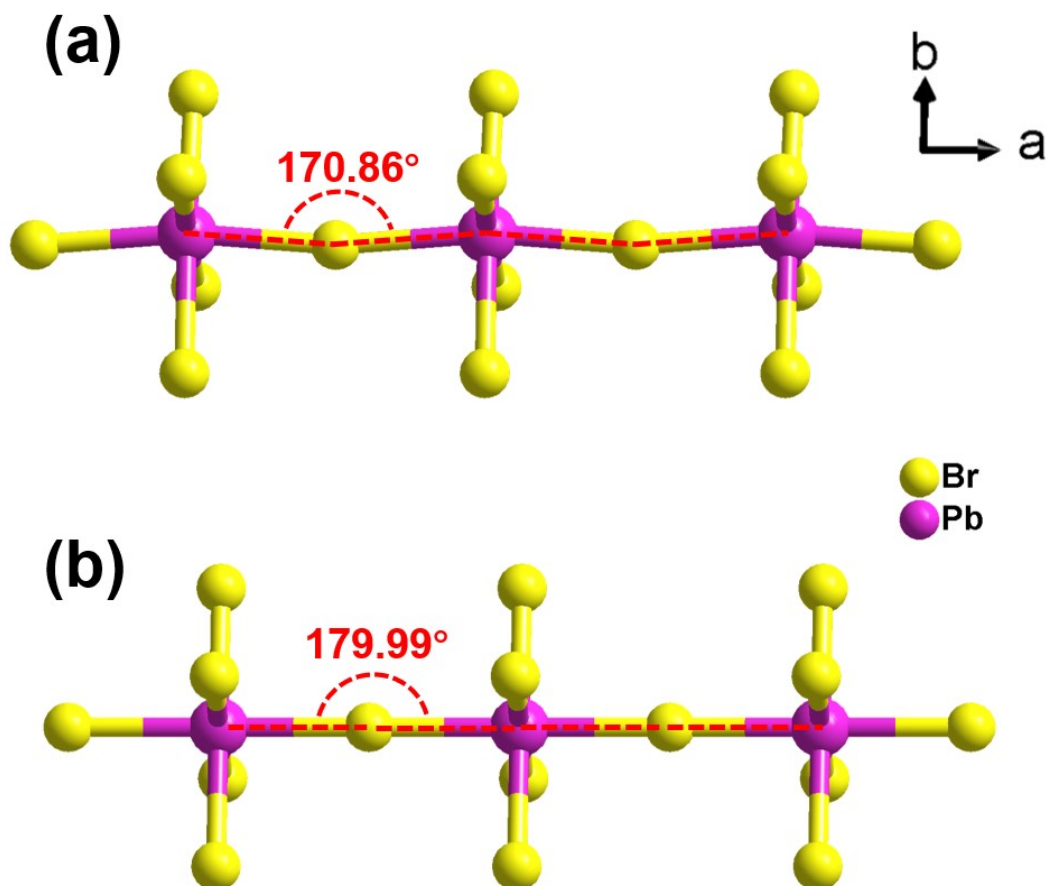


Fig. S3 The coordination geometry of $[\text{PbBr}_5]^{3-}$ infinite 1D anionic chains at (a) 120 K and (b) 273 K.

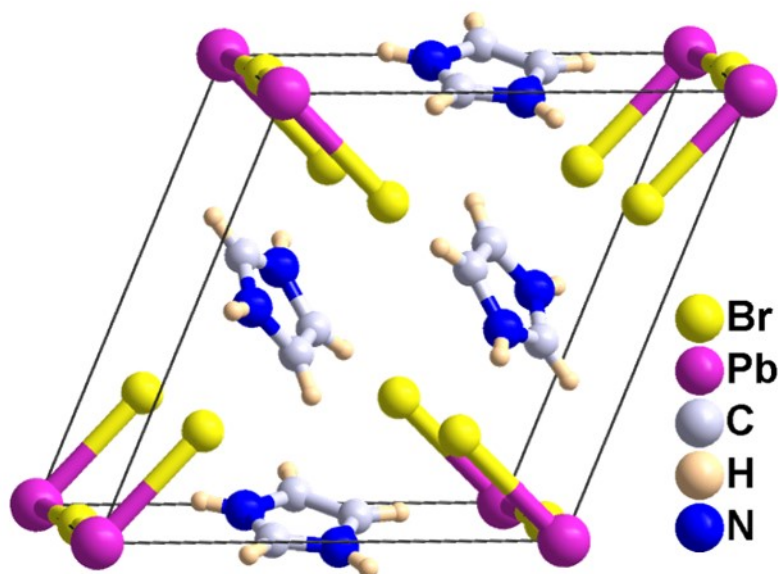


Fig. S4 The point charge model for IM_3PbBr_5 at 120 K in LTP.

According to the crystal structure data collected at 120 K, we select a unit cell and assume that the centers of the positive charges of the Imidazolium cations are located on the N atoms. The negative charges and positive charges of the $(\text{PbBr}_3)^{3-}$ chains are located on the Br atoms and Pb atoms, respectively.

Atoms	Coordinate of charge center
N	(0.48638, 0.54101, 0.49291)
Br	(0.50452, 0.49528, 0.50254)
Pb	(0.50000, 0.50000, 0.50000)

a-axis:

$$\begin{aligned}
 P_s &= \lim_{\bar{V}} \frac{1}{\bar{V}} \sum q_i r_i \\
 &= (q_N r_N + q_{\text{Pb}} r_{\text{Pb}} + q_{\text{Br}} r_{\text{Br}}) / V \\
 &= [(e \times 3 \times 0.48638) + (e \times 2 \times 0.5) + (-e \times 5 \times 0.50452)] \times a / V \\
 &= [0.06346 \times 1.602 \times 10^{-19} \times 5.9809 \times 10^{-10} \text{ C m}] / (491.29 \times 10^{-30} \text{ m}^3) \\
 &= 1.24 \times 10^{-2} \text{ C m}^{-2} \\
 |P_s| &= 1.24 \times 10^{-2} \text{ C m}^{-2} = 1.24 \mu\text{C cm}^{-2}
 \end{aligned}$$

b-axis:

$$\begin{aligned}
 P_s &= \lim_{\bar{V}} \frac{1}{\bar{V}} \sum q_i r_i \\
 &= (q_N r_N + q_{\text{Pb}} r_{\text{Pb}} + q_{\text{Br}} r_{\text{Br}}) / V \\
 &= [(e \times 3 \times 0.54101) + (e \times 2 \times 0.5) + (-e \times 5 \times 0.49528)] \times b / V \\
 &= [0.14663 \times 1.602 \times 10^{-19} \times 9.3967 \times 10^{-10} \text{ C m}] / (491.29 \times 10^{-30} \text{ m}^3) \\
 &= 4.49 \times 10^{-2} \text{ C m}^{-2} \\
 |P_s| &= 4.49 \times 10^{-2} \text{ C m}^{-2} = 4.49 \mu\text{C cm}^{-2}
 \end{aligned}$$

c-axis:

$$\begin{aligned}
 P_s &= \lim_{\bar{V}} \frac{1}{\bar{V}} \sum q_i r_i \\
 &= (q_N r_N + q_{\text{Pb}} r_{\text{Pb}} + q_{\text{Br}} r_{\text{Br}}) / V \\
 &= [(e \times 3 \times 0.49291) + (e \times 2 \times 0.5) + (-e \times 5 \times 0.50254)] \times c / V \\
 &= [0.03397 \times 1.602 \times 10^{-19} \times 9.5001 \times 10^{-10} \text{ C m}] / (491.29 \times 10^{-30} \text{ m}^3) \\
 &= 1.05 \times 10^{-2} \text{ C m}^{-2} \\
 |P_s| &= 1.05 \times 10^{-2} \text{ C m}^{-2} = 1.05 \mu\text{C cm}^{-2}
 \end{aligned}$$

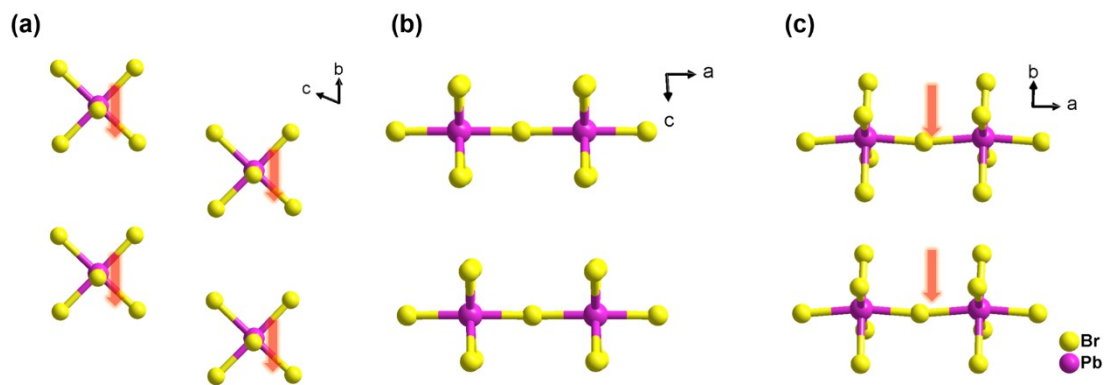


Fig. S5 The packing view of $[\text{PbBr}_5]^{3-}$ infinite 1D anionic chains along (a) a -axis, (b) b -axis and (c) c -axis.

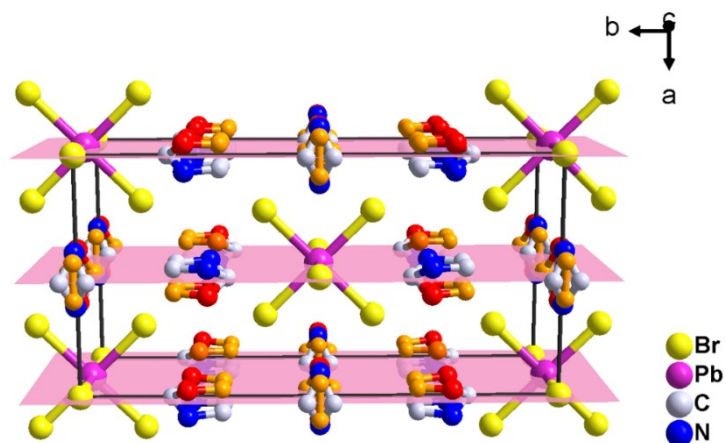


Fig. S6 The packing view of IM_3PbBr_5 at 405 K. The pink plane represents the mirror perpendicular to the a -axis.

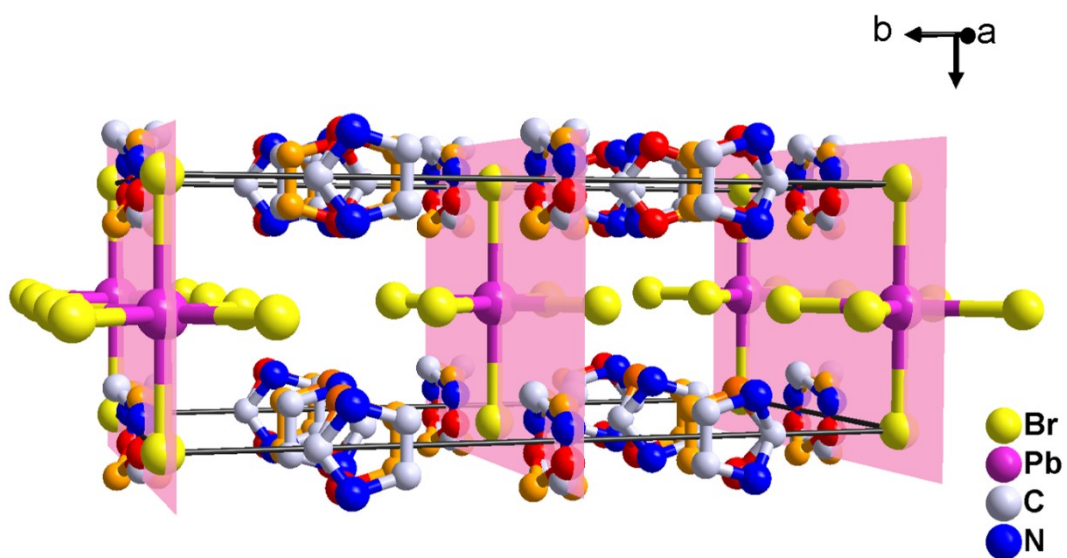


Fig. S7 The packing view of IM_3PbBr_5 at 405 K. The pink plane represents the mirror

perpendicular to the *b*-axis.

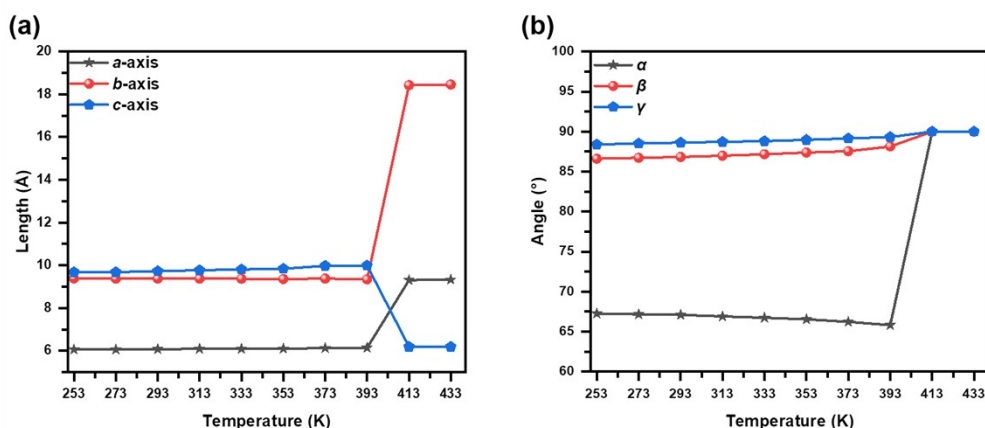


Fig. S8 Temperature-dependent unit-cell parameters of IM₃PbBr₅. (a) Unit-cell length and (b) unit-cell angle.

Table S1. Crystal data and structure refinements for IM₃PbBr₅ at 120 K, 273 K and 405 K.

	LTP (120 K)	ITP (273 K)	HTP (405 K)
Empirical formula	(C ₃ H ₅ N ₂) ₃ PbBr ₅	(C ₃ N ₂) ₃ PbBr ₅	(C ₃ N ₂) ₃ PbBr ₅
Formula weight	814.01	798.89	798.89
Space group	<i>P</i> 1	<i>P</i> $\bar{1}$	<i>Cmmm</i>
Crystal system	Triclinic	Triclinic	Orthorhombic
a/ Å	5.9809 (2)	6.0580 (11)	9.3390 (6)
b/ Å	9.3967 (3)	9.3771 (19)	18.4650 (12)
c/ Å	9.5001 (3)	9.7010 (2)	6.2010 (3)
α/°	67.3760 (10)	67.101 (6)	90
β/°	85.6790 (10)	86.784 (6)	90
γ/°	87.1050 (10)	88.497 (5)	90
Volume/ Å³	491.29 (3)	506.86 (18)	1069.4 (11)
Z	1	1	2
F(000)	368	353	706
GOF	1.030	1.072	1.081
R_{int}	0.0676	0.0951	0.1104
R₁	0.0360	0.0431	0.0419
wR₂	0.0800	0.1014	0.1280

Table S2. Selected bond lengths [Å] and bond angles for IM₃PbBr₅ at 120 K.

bond lengths [Å]		bond angles [°]	
Br1—Pb1	3.0595 (13)	Pb1—Br5—Pb1i	170.86 (4)
Br2—Pb1	3.0113 (14)	Br2—Pb1—Br1	88.52 (4)
Br3—Pb1	3.0059 (14)	Br2—Pb1—Br5ii	87.18 (4)
Br4—Pb1	2.9737 (13)	Br3—Pb1—Br1	178.47 (6)
Br5—Pb1i	3.0325 (15)	Br3—Pb1—Br2	91.91 (4)

Br5—Pb1	2.9675 (15)	Br3—Pb1—Br5ii	86.72 (4)
		Br4—Pb1—Br1	90.42 (4)
		Br4—Pb1—Br2	178.05 (5)
		Br4—Pb1—Br3	89.11 (4)
		Br4—Pb1—Br5ii	94.53 (4)
		Br5—Pb1—Br1	90.73 (4)
		Br5ii—Pb1—Br1	94.77 (4)
		Br5—Pb1—Br2	85.67 (4)
		Br5—Pb1—Br3	87.83 (4)
		Br5—Pb1—Br4	92.72 (4)
		Br5—Pb1—Br5ii	170.86 (4)

Symmetry codes: (i) $x+1, y, z$; (ii) $x-1, y, z$.

Table S3. Selected bond lengths [\AA] and bond angles for IM_3PbBr_5 at 273 K.

bond lengths [\AA]		bond angles [$^\circ$]	
Br1—Pb1	3.0045 (8)	Pb1i—Br3—Pb1	180.0
Br2—Pb1	3.0319 (8)	Br1—Pb1—Br1iii	180.0
Br3—Pb1i	3.0290 (5)	Br1iii—Pb1—Br2	88.35 (2)
Br3—Pb1	3.0290 (5)	Br1—Pb1—Br2	91.65 (2)
		Br1—Pb1—Br2iii	88.35 (2)
		Br1iii—Pb1—Br2iii	91.65 (2)
		Br1—Pb1—Br3iv	89.837 (14)
		Br1—Pb1—Br3	90.163 (14)
		Br1iii—Pb1—Br3	89.837 (14)
		Br1iii—Pb1—Br3iv	90.163 (14)
		Br2iii—Pb1—Br2	180.0
		Br3—Pb1—Br2	88.560 (13)
		Br3—Pb1—Br2iii	91.440 (13)
		Br3iv—Pb1—Br2iii	88.560 (13)
		Br3iv—Pb1—Br2	91.440 (13)
		Br3iv—Pb1—Br3	180.0

Symmetry codes: (i) $x-1, y, z$; (ii) $-x+2, -y, -z+1$; (iii) $-x+1, -y+1, -z+1$; (iv) $x+1, y, z$.

Table S4. Selected bond lengths [\AA] and bond angles for IM_3PbBr_5 at 405 K.

bond lengths [\AA]		bond angles [$^\circ$]	
Pb01—Br02	3.1005 (16)	Br02i—Pb01—Br02	180.0
Pb01—Br02i	3.1005 (16)	Br03—Pb01—Br02	90.0
Pb01—Br03ii	3.032 (2)	Br03—Pb01—Br02i	90.0
Pb01—Br03iii	3.032 (2)	Br03iii—Pb01—Br02i	90.0
Pb01—Br03iv	3.032 (2)	Br03ii—Pb01—Br02	90.0
Pb01—Br03	3.032 (2)	Br03iv—Pb01—Br02	90.0
		Br03ii—Pb01—Br02i	90.0

Br03iv—Pb01—Br02i	90.0
Br03iii—Pb01—Br02	90.0
Br03—Pb01—Br03iv	89.00 (8)
Br03—Pb01—Br03ii	91.00 (8)
Br03—Pb01—Br03iii	180.0
Br03iii—Pb01—Br03iv	91.01 (8)
Br03iii—Pb01—Br03ii	88.99 (8)
Br03ii—Pb01—Br03iv	180.0
Pb01xii—Br02—Pb01	180.0

Symmetry codes: (i) $x, y, z+1$; (ii) $x, -y+1, z$; (iii) $-x+1, -y+1, -z+1$; (iv) $-x+1, y, -z+1$; (v) $-x+1, y, z$; (vi) $-x+1, y, -z$; (vii) $x, y, -z$; (viii) $-x+1, -y, -z$; (ix) $x, -y, -z$; (x) $-x+1, -y, z$; (xi) $x, -y, z$; (xii) $x, y, z-1$.

Table S5. The comparison of saturated polarization (P_s) in reported one-dimensional organic–inorganic lead-based ferroelectrics.

Compound	P_s ($\mu\text{C cm}^{-2}$)	Ref
[4'-nitrobenzylidene-1-aminopyridinium][PbBr ₃]	3.45	1
[(CH ₃) ₃ NCH ₂ I]PbI ₃	0.67	2
(R)-(-)-1-cyclohexylethylammonium)PbI ₃	1.2	3
(S)-(+)-1-cyclohexylethylammonium)PbI ₃	1.2	3
IM ₃ PbBr ₅	4.54	This work

Reference:

1. S.-P. Zhao, Y. Guo, J. Wang, H. Xu, Q. Qiao and R.-Y. Huang, An inorganic-organic hybrid compound with face-sharing bromoplumbate chain: Synthesis, crystal structure, Hirshfeld surface analysis, ferroelectric and dielectric properties, *Polyhedron*, 2020, **178**, 114345.
2. X. N. Hua, W. Q. Liao, Y. Y. Tang, P. F. Li, P. P. Shi, D. Zhao and R. G. Xiong, A Room-Temperature Hybrid Lead Iodide Perovskite Ferroelectric, *J. Am. Chem. Soc.*, 2018, **140**, 12296-12302.
3. Y. Hu, F. Florio, Z. Chen, W. A. Phelan, M. A. Siegler, Z. Zhou, Y. Guo, R. Hawks, J. Jiang, J. Feng, L. Zhang, B. Wang, Y. Wang, D. Gall, E. F. Palermo, Z. Lu, X. Sun, T.-M. Lu, H. Zhou, Y. Ren, E. Wertz, R. Sundararaman and J. Shi, A chiral switchable photovoltaic ferroelectric 1D perovskite, *Science Advances*, 2020, **6**, eaay4213.